ISSN 1070-3284, Russian Journal of Coordination Chemistry, 2015, Vol. 41, No. 6, pp. 376–386. © Pleiades Publishing, Ltd., 2015.
Original Russian Text © A.S. Burlov, S.A. Mashchenko, V.G. Vlasenko, K.A. Lysenko, A.S. Antsyshkina, G.G. Sadikov, V.S. Sergienko, Yu.V. Koshchienko, Ya.V. Zubavichus, A.I. Uraev, D.A. Garnovskii, E.V. Korshunova, S.I. Levchenkov, 2015, published in Koordinatsionnaya Khimiya, 2015, Vol. 41, No. 6, pp. 346–356.

Metal Complexes of Azomethine Compounds Bearing an Azo Group in the Amine Fragment: Syntheses, Structures, and Properties

A. S. Burlov[a, *], S. A. Mashchenko[a], V. G. Vlasenko[b], K. A. Lysenko[c], A. S. Antsyshkina[d], G. G. Sadikov[d], V. S. Sergienko[d], Yu. V. Koshchienko[a], Ya. V. Zubavichus[c, e], A. I. Uraev[a], D. A. Garnovskii[a, f], E. V. Korshunova[a], and S. I. Levchenkov[f]

[a] *Research Institute of Physical and Organic Chemistry, Southern Federal University, Rostov-on-Don, Russia*

[b] *Research Institute of Physics, Southern Federal University, Rostov-on-Don, Russia*

[c] *Nesmeyanov Institute of Organoelement Compounds, Russian Academy of Sciences, ul. Vavilova 28, Moscow, 119991 Russia*

[d] *Kurnakov Institute of General and Inorganic Chemistry, Russian Academy of Sciences, Leninskii pr. 31, Moscow, 119991 Russia*

[e] *Kurchatov Institute Russian Research Center, pl. Kurchatova 1, Moscow, 123182 Russia*

[f] *Southern Scientific Center, Russian Academy of Sciences, Rostov-on-Don, Russia*

**e-mail: anatoly.burlov@yandex.ru*

Received December 8, 2014

Abstract—New complexes of Cu(II), Co(II), Ni(II), and Zn(II) with 1-phenyl-3-methyl-4-(4-phenylazophenylaminomethylene)pyrazol-5-one (HL^1) and 1-phenyl-3-methyl-4-[4-methyl-2-(4-methylphenylazo)phenylaminomethylene]pyrazol-5-one (HL^2) are synthesized using chemical and electrochemical methods and characterized by IR spectroscopy, ^{1}H NMR spectroscopy, X-ray absorption spectroscopy, X-ray diffraction analysis, and magnetic measurements. All complexes are mononuclear. The structures of HL^2 and related cobalt complex are determined by X-ray diffraction analysis (CIF files CCDC nos. 1028957 and 1035847, respectively).

DOI: 10.1134/S1070328415060019

INTRODUCTION

Coordination compounds of azomethine ligands are important objects of the modern chemistry of metal complexes and are considered in a series of monographs and reviews [1–9].

An increased attention to complexes of azomethine compounds is due to the possibility of a wide variation of their ligand environment presented by aldehyde and amine moieties (molecular design) [7, 9] and the production of multifunctional materials from these compounds. Among such materials are magnetoactive [8, 10, 11] and luminescent [12] complexes and chemosensors [13–15]. Complexes of azomethine ligands are also widely presented among biocoordination systems [16, 17].

An important role in the investigation of molecular magnetic materials and systems exhibiting the thermo- and photoinduced crossover effect [18, 19] belongs to the study of the coordination compounds of azomethines containing an azobenzene moiety that is not involved in coordination with the metal [20, 21]. Its ability to undergo photoinduced *E/Z* isomerization is significant for the development of coordination compounds with the properties of molecular switchers [22]. The *E/Z* isomerization of the azobenzene fragment is applied for the formation of metastable nanoparticles used in the reversible process of image recording/clearing [23].

In this work, we present the results of chemical (CS) and electrochemical (ECS) syntheses, IR spectroscopy, ^{1}H NMR spectroscopy, XAFS and X-ray diffraction analyses, and magnetochemical study of the Cu(II), Co(II), Ni(II), and Zn(II) chelates of azomethine compounds of 1-phenyl-3-methyl-4-formyl-5-pyrazolone with aminoazobenzenes containing an azo group in the *para* (HL^1) and *ortho* (HL^2) positions of the amine fragment (**Ia–Id** and **IIa–IId**, respectively).

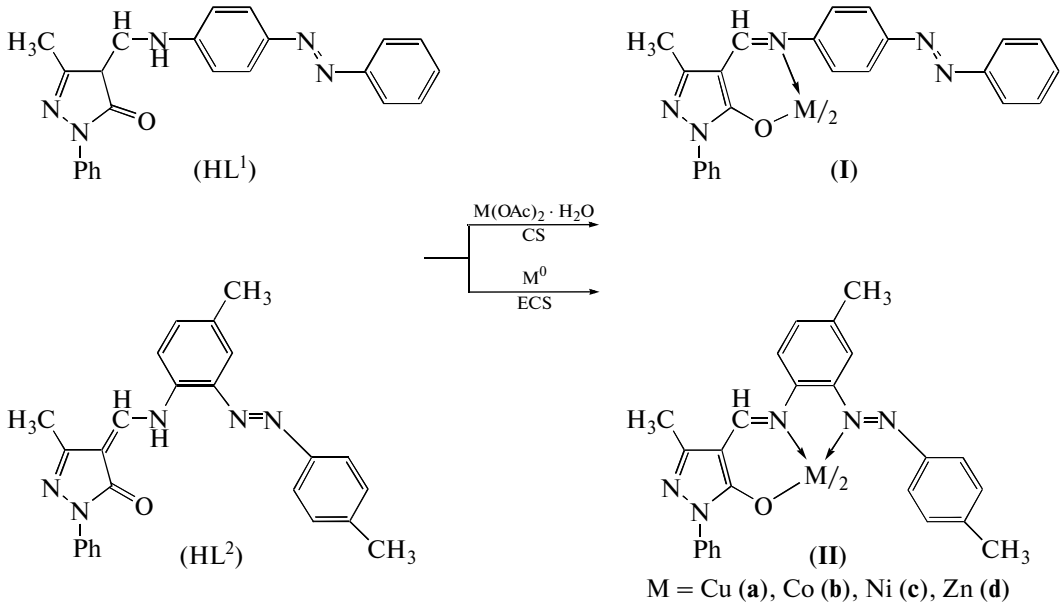

Scheme 1.

EXPERIMENTAL

Commercially available 4-aminoazobenzene, 6-amino-4,4'-dimethylazobenzene, and 3-methyl-1-phenylpyrazol-5-one were used.

1-Phenyl-3-methyl-4-formyl-5-pyrazolone was synthesized using a known procedure [24].

Syntheses of HL^1 and HL^2. A solution of 4-aminobenzene (HL^1) (3.94 g, 0.02 mol) or 6-amino-4,4'-dimethylazobenzene (HL^2) (4.5 g, 0.02 mol) was added to a solution of 1-phenyl-3-methyl-4-formyl-5-pyrazolone (4.04 g, 0.02 mol) in benzene (15 mL). The obtained mixture was refluxed with the Dean–Stark trap for 4 h until the complete separation of water. After the end of the reaction, the solvent was distilled off on a rotary evaporator to 1/4 of the volume. The precipitates of azomethines were filtered off and recrystallized from an ethanol–chloroform (2 : 1) mixture.

Compound HL^1, 1-phenyl-3-methyl-4-(4-phenylazophenylaminomethylene)pyrazol-5-one, formed in a yield of 86%, was represented by red crystals with mp = 198–199°C.

IR (ν, cm^{-1}): 3041 (NH), 1657 (C=O). ^1H NMR ($CDCl_3$, δ, ppm): 2.32 s (3H, CH_3), 7.16 t (1H, C_{Ar}–H, J = 7.8 Hz), 7.31–7.51 t (7H, C_{Ar}–H), 7.88–8.01 t (7 H, C_{Ar}–H, =<u>CH</u>–NH–), 11.63 br.s (1 H, NH).

For $C_{23}H_{19}N_5O$			
anal. calcd., %:	C, 72.43;	H, 5.03;	N, 18.36.
Found, %:	C, 72.67;	H, 4.87;	N, 18.22.

Compound HL^2, 1-phenyl-3-methyl-4-[4-methyl-2-(4-methylphenylazo)phenylaminomethylene]pyrazol-5-one, formed in a yield of 99%, was represented by red crystals with mp = 220–221°C.

IR (ν, cm^{-1}): 3059 (NH), 1660 (C=O). ^1H NMR ($CDCl_3$, δ, ppm): 2.31 s (3H, CH_3), 2.38 s. (3H, CH_3), 2.44 s. (3H, CH_3), 7.14 t (1H, C_{Ar}–H, J = 7.4 Hz) 7.26–7.44 m (6H, C_{Ar}–H), 7.68 s. (1H, C_{Ar}–H), 7.97 d (1H, =<u>CH</u>–NH–, J = 12.8 Hz), 8.06–8.14 m (4H, C_{Ar}–H), 12.90 d (1H, =CH–<u>NH</u>–, J = 12.4 Hz).

For $C_{25}H_{23}N_5O$			
anal. calcd., %:	C, 77.33;	H, 5.66;	N, 17.10.
Found, %:	C, 77.34;	H, 5.47;	N, 16.98.

Single crystals of HL^2 suitable for X-ray diffraction analysis were grown from a chloroform–methanol (1 : 2) mixture.

Chemical synthesis of complexes I and II. A solution of the corresponding metal acetate hydrate (0.5 mmol) in methanol (10 mL) was poured to a solution of HL^1 or HL^2 (1 mmol) in a chloroform–methanol (1 : 2) mixture (20 mL). The mixture was refluxed for 1 h. Brown precipitates of the complexes formed after cooling were filtered off, washed with methanol, and recrystallized from a chloroform–methanol (1 : 2) mixture.

Electrochemical synthesis of complexes I and II. A solution of HL^1 or HL^2 (1 mmol) in methanol (20 mL) and $[Et_4N]ClO_4$ (0.01 g) as a current-conducting additive were placed in an electrochemical cell with a platinum cathode and an anode of a complexing metal (Co, Ni, Cu, or Zn). Electrosynthesis was carried out

at a constant current strength of 40 mA and a voltage of 15 V for 1 h. Dark red precipitates of the complexes were filtered off, washed with methanol, and recrystallized from a chloroform–methanol (1 : 2) mixture.

Complex **Ia**, copper(II) bis{1-phenyl-3-methyl-4[(4-phenylazo)phenylaminomethylene]pyrazol-5-onate}, formed in a yield of 89%, was a brown powder with mp > 250°C and μ_{eff} = 2.09 μ_B (294 K). IR (ν, cm^{-1}): 1613(CH=N).

For $C_{46}H_{36}N_{10}O_2Cu$

anal. calcd., %: C, 67.02; H, 4.40; N, 16.99; Cu, 7.71.
Found (CS), %: C, 67.09; H, 4.42; N, 16.85; Cu, 7.79.
Found (ECS), %: C, 67.11; H, 4.39; N, 16.79; Cu, 7.85.

Complex **Ib**, cobalt(II) bis{1-phenyl-3-methyl-4[(4-phenylazo)phenylaminomethylene]pyrazol-5-onate}, formed in a yield of 61%, was represented by red crystals with mp > 250°C and μ_{eff} = 4.01 μ_B (294 K). IR (ν, cm^{-1}): 1607 (CH=N).

For $C_{46}H_{36}N_{10}O_2Co$

anal. calcd., %: C, 67.40; H, 4.43; N, 17.08; Co, 7.19.
Found (CS), %: C, 67.38; H, 4.45; N, 17.12; Co, 7.15.
Found (ECS), %: C, 67.26; H, 4.51; N, 17.19; Co, 7.21.

Complex **Ic**, nickel(II) bis{1-phenyl-3-methyl-4[(4-phenylazo)phenylaminomethylene]pyrazol-5-onate}, formed in a yield of 75%, was represented by brown crystals with mp > 250°C and μ_{eff} = 3.09 μ_B (294 K). IR (ν, cm^{-1}): 1616(CH=N).

For $C_{46}H_{36}N_{10}O_2Ni$

anal. calcd., %: C, 67.42; H, 4.43; N, 17.09; Ni, 7.16.
Found (CS), %: C, 67.39; H, 4.42; N, 17.06; Ni, 7.19.
Found (ECS), %: C, 67.45; H, 4.38; N, 17.13; Ni, 7.18.

Complex **Id**, zinc(II) bis{1-phenyl-3-methyl-4[(4-phenylazo)phenylaminomethylene]pyrazol-5-onate}, formed in a yield of 73%, was represented by orange crystals with mp > 250°C. IR (ν, cm^{-1}): 1611 (CH=N). ^{1}H NMR ($CDCl_3$, δ, ppm): 2.37 s (3H, CH_3), 713–7.24 m (4H, C_{Ar}–H), 7.37–7.48 m (5H, C_{Ar}–H), 7.82–7.87 m (4H, C_{Ar}–H), 7.95–7.99 m (2H, C_{Ar}–H) 8.30 s (1H, CH=N).

For $C_{46}H_{36}N_{10}O_2Zn$

anal. calcd., %: C, 66.87; H, 4.39; N, 16.95; Zn, 7.91.
Found (CS), %: C, 66.79; H, 4.35; N, 17.01; Zn, 7.89.
Found (ECS), %: C, 66.71; H, 4.39; N, 17.09; Zn, 7.88.

Complex **IIa**, copper(II) bis{1-phenyl-3-methyl-4-[4-methyl-2-(4-methylphenylazo)phenylaminomethylene]pyrazol-5-onate}, formed in a yield of 72%, was represented by brown crystals with mp > 250°C and μ_{eff} = 1.89 μ_B (294 K). IR (ν, cm^{-1}): 1614 (CH=N).

For $C_{50}H_{44}N_{10}O_2Cu$

anal. calcd., %: C, 68.21; H, 5.04; N, 15.91; Cu, 7.22.
Found (CS), %: C, 68.29; H, 5.07; N, 15.96; Cu, 7.19.
Found (ECS), %: C, 68.27; H, 5.11; N, 15.87; Cu, 7.13.

Complex **IIb**, cobalt(II) bis{1-phenyl-3-methyl-4-[4-methyl-2-(4-methylphenylazo)phenylaminomethylene]pyrazol-5-onate}, formed in a yield of 74%, was represented by brown crystals with mp > 250°C and μ_{eff} = 4.12 μ_B (294 K). IR (ν, cm^{-1}): 1622 (CH=N).

For $C_{50}H_{44}N_{10}O_2Co$

anal. calcd., %: C, 68.56; H, 5.06; N, 15.99; Co, 6.73.
Found (CS), %: C, 68.47; H, 5.01; N, 15.96; Co, 6.81.
Found (ECS), %: C, 68.37; H, 5.01; N, 15.88; Co, 6.89.

Single crystals of complex **IIb** suitable for X-ray diffraction analysis were grown from dimethylformamide.

Complex **IIc**, nickel(II) bis{1-phenyl-3-methyl-4-[4-methyl-2-(4-methylphenylazo)phenylaminomethylene]pyrazol-5-onate}, formed in a yield of 78%, was represented by red crystals with mp > 250°C and μ_{eff} = 3.09 μ_B(294 K). IR (ν, cm^{-1}): 1620 (CH=N).

For $C_{50}H_{44}N_{10}O_2Ni$

anal. calcd., %: C, 68.58; H, 5.06; N, 15.90; Ni, 6.70.
Found (CS), %: C, 68.51; H, 5.09; N, 15.97; Ni, 6.74.
Found (ECS), %: C, 68.43; H, 5.10; N, 15.97; Ni, 6.74.

Elemental analyses to C, H, and N were carried out on a Carlo Erba Instruments TCM 480 instrument. The metal content was analyzed by the gravimetric method. Attenuated total internal reflectance powder IR spectra were recorded on a Varian Excalibur-3100 FT–IR instrument. ^{1}H NMR spectra were measured on a Varian Unity-300 instrument (300 MHz) in the internal stabilization mode of the ^{2}H polar resonance line in $CDCl_3$.

X-ray absorption Cu, Co, and Ni *K*-edge spectra for compounds **I** and **II** were obtained on the Structural Materials Science station at the Kurchatov Center of Synchrotron Radiation and Nanotechnologies (Moscow) [25]. The energy of the electron beam used as an X-ray synchrotron radiation source was 2.5 GeV at a current of 60–80 mA. A double crystal monochromator Si(111) was used for X-ray radiation monochromatization. The X-ray beam intensity before and after the irradiation of a sample was measured using two ionization chambers filled with nitrogen–argon mixtures giving 20 and 80% absorption for I_0 and I_t, respectively.

The obtained X-ray absorption spectra were processed using standard procedures of background subtraction, normalization to the value of the *K*-edge jump, and the isolation of atomic absorption μ_0 [26], after which the Fourier transform of the obtained extended X-ray absorption fine structure (EXAFS) χ spectra was performed in the range of photoelectron wave vectors k from 2.6 to 12–13 Å^{-1} with the weight function k^3. The obtained module Fourier transformants (MFT) of the χ spectra corresponded to the radial distribution function of the atoms around the absorbing metal atom with the phase shift accuracy. The threshold ionization energy (E_0) was chosen by the value of the maximum of the first derivative of the *K* edge and further was varied by fitting.

The exact values for parameters of the nearest environment of the metal atoms in the metal complexes were determined by the nonlinear fitting of the parameters of the coordination spheres comparing the calculated EXAFS signal and the signal isolated from the full EXAFS spectrum by the Fourier filtration method. The nonlinear fitting was performed using the IFFEFIT program package [27]. The phases and scattering amplitudes of the photoelectron wave necessary for the construction of the model spectrum were calculated using the FEFF7 program [28]. The X-ray structural data for single crystals of the complexes with the similar atomic environment of the metal atoms were used as the initial atomic coordinates necessary for the calculation of the phases and scattering amplitudes and subsequent fitting. The search for these structures was performed in the Cambridge Crystallographic Data Centre (CCDC).

The goodness-of-fit Q, which was minimized when determining the parameters of the nearest environment structure, was calculated by the formula

$$Q = \frac{\sum[k\chi_{exp}(k) - k\chi_{th}(k)]^2}{\sum[k\chi_{exp}(k)]^2} \times 100\%.$$

X-ray diffraction analysis. The experimental material for the examination of crystals of HL^2 was obtained on an Enraf-Nonius Cad-4 diffractometer (4 (MoK_α radiation, graphite monochromator). The X-ray diffraction analysis of complex **IIb** was carried out on a Bruker SMART APEX II diffractometer equipped with a CCD detector and a monochromatic radiation source (MoK_α, $\lambda = 0.71073$ Å) using a standard procedure [29]. An absorption correction was applied semiempirically [30]. The structures were solved by a direct method and refined in the full-matrix anisotropic approximation for all non-hydrogen atoms. Hydrogen atoms were generated geometrically and refined in the riding model. The calculations were performed using the SHELXS-97 and SHELXL-97 programs [31]. The PLATON program was used for an analysis of the geometry of molecules [32].

The experimental material for studying HL^2 was obtained from the sample containing a minor impurity of the twin variant. The crystallographic parameters and X-ray diffraction experimental data for HL^2 and **IIb** are given in Table 1. The coordinates of atoms and temperature factors were deposited with the Cambridge Crystallographic Data Centre (CCDC 1028957 (HL^2) and 1035847 (**IIb**); deposit@ccdc.cam.ac.uk or http://www.ccdc.cam.ac.uk).

The specific magnetic susceptibility in the solid phase was determined by the relative Faraday method in the temperature range 77.4–300 K using $Hg[Co(CNS)_4]$ as a standard for calibration [33].

RESULTS AND DISCUSSION

Compounds HL^1 and HL^2 and related metal complexes were synthesized to extend the range of compounds with potential photoinduced changes in the magnetic properties due to the isomerization of the peripheral azo groups in the combined azo–azomethine complexes and to continue our earlier studies [34–37]. The structures of HL^1 and HL^2 were determined by ^{1}H NMR spectroscopy. It is known [38–40] that the equilibrium of tautomers (**a–d**) can take place in compounds HL^1 and HL^2

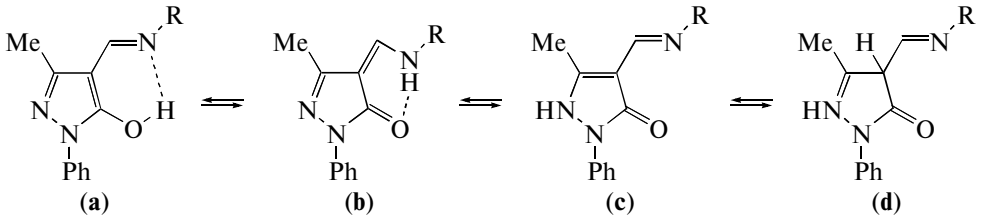

Scheme 2.

The ^{1}H NMR spectrum of HL^1 contains doublet signals of the =CH–NH= protons at 8.14 ppm (J = 11.4 Hz) and doublet signals of the NH protons at 13.67 ppm (J = 12.1 Hz). Similar signals of protons

Table 1. Crystallographic data and the experimental and refinement characteristics for compounds HL^2 and **IIb**

Parameter	Value	
	HL^2	**IIb**
Empirical formula	$C_{25}H_{23}N_5O$	$C_{50}H_{44}CoN_{10}O_2$
FW	409.48	875.88
Crystal size, mm	0.04 × 0.03 × 0.03	0.25 × 0.20 × 0.20
Temperature	293(2)	100(2)
Crystal system	Monoclinic	Orthorhombic
Space group	$P2_1/n$	$P2_12_12_1$
a, Å	7.9886(10)	12.5550(9)
b, Å	10.6963(10)	14.1511(11)
c, Å	25.5566(10)	24.0148(18)
β, deg	97.209(10)	90
V, Å^3	2166.5(3)	4266.6(6)
Z	4	4
ρ(calcd), g/cm^3	1.255	1.364
μ, mm^{-1}	0.080	0.457
F(000)	864	1828
Scan range θ, deg	2.07–29.96	1.67–29.00
Reflection index range	$-9 \le h \le 9$, $0 \le k \le 14$, $-35 \le l \le 35$	$-17 \le h \le 16$, $-19 \le k \le 19$, $-32 \le l \le 32$
Number of measured reflections	12131	46562
Number of independent reflections	6072	11291
Number of reflections with $I \ge 2\sigma(I)$	1284	8499
Number of refined parameters	349	574
Goodness-of-fit (all reflections)	0.872	0.891
R_1 ($I > 2\sigma(I)$)	0.0808	0.0373
wR_2 (all reflections)	0.3060	0.0469
$\Delta\rho_{max}/\Delta\rho_{min}$, *e* Å^{-3}	0.152/–0.136	0.900/–0.625

appear in the spectrum of compound HL^2. The IR spectra of these compounds exhibit stretching vibration bands of the C=O (1657–1662 cm^{-1}) and NH (3041–3058 cm^{-1}) groups. These spectral characteristics indicate that the aminomethylene tautomeric form (**b**) takes place in compounds HL^1 and HL^2 (Scheme 2), which is confirmed by the X-ray diffraction data for HL^2 (Fig. 1).

In the crystalline state, HL^2 exists in the aminomethylene tautomeric form, which is indicated by the short interatomic distance C(9)–O(1) 1.237(2) Å in the pyrazolone fragment corresponding to the double bond [41]. This form is stabilized by a fairly strong intramolecular hydrogen bond N(3)–H(3*A*)···O(1) (N(3)–H(3*A*) 0.86, H(3*A*)···O(1) 2.13, N(3)···O(1) 2.808(6) Å, N(3)H(3*A*)O(1) 136°). In addition, there is the hydrogen bond N(3)–H(3*A*)···N(4) (N(3)–H(3*A*) 0.86, H(3*A*)···N(4) 2.25, N(3)···N(4) 2.625(7) Å, N(3)H(3*A*)N(4) 106°).

A molecule of HL^2 is not planar. The C(11)–C(16) cycle is turned relatively to the pyrazole cycle N(1)N(2)C(7)C(9) along the N(3)–C(11) bond by 17.33°. The phenyl cycle C(1)–C(6) is nearly coplanar to the pyrazole cycle (the dihedral angle between the mean planes is 3.82°).

The structure can be presented as two significantly planar fragments C(1)–C(11) and C(11)–C(22) linked by the common C(11) atom (Fig. 1). The dihedral angle between these planes is 27.6°. The C(1)–C(11) group is planar within 3.5°. In the C(11)–C(22) fragment, two planar cycles C(11)–C(16) and C(17)–C(22) linked by the N(4)–N(5) bridge are unfolded relatively to each other by 10.3°. The torsion angle C(16)N(4)N(5)C(17) is 177.3°.

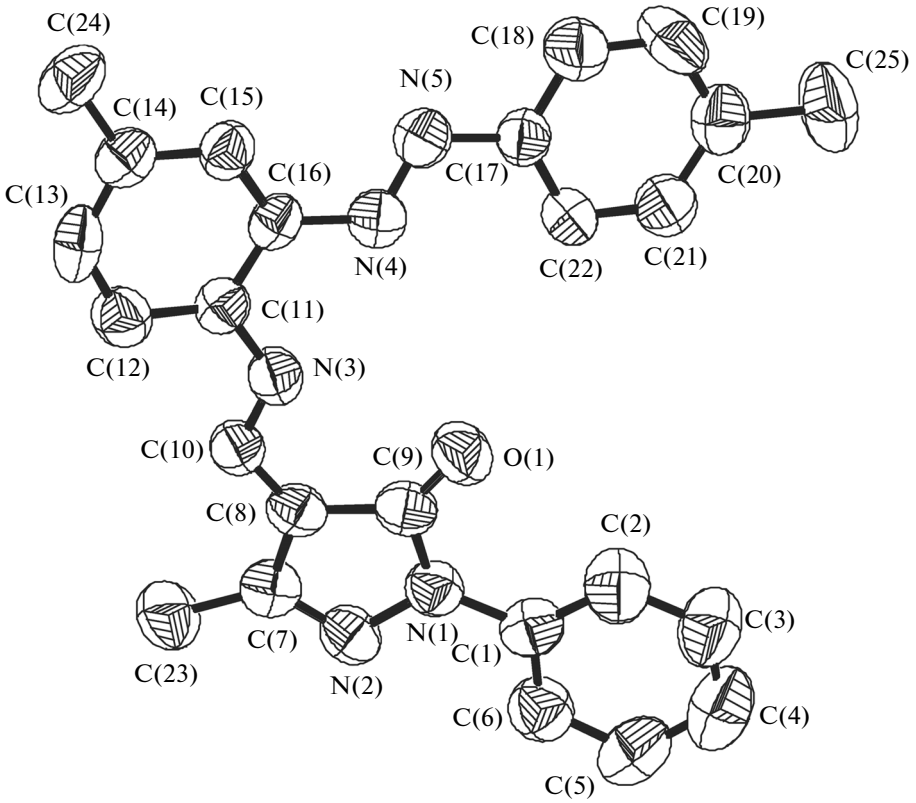

Fig. 1. Structure of molecule HL_2 in the representation of atoms by 50% probability atomic displacement ellipsoids.

Molecule HL^2 enters the composition of octahedral complex **IIb** as a ligand, where HL^2 participates in the formation of the *trans*-meridional isomer.

On going from the ligand systems to complexes **I** and **II**, the changes characteristic of chelate structures occur in the IR spectra: the ν(NH) absorption band frequencies of the ligand (3041–3058 cm^{-1}) disappear and the ν(C=N) absorption bands appear at 1607–1616 cm^{-1}.

In the ^1H NMR spectra of zinc complexes **Id** obtained by the CS ad ECS, the signals from the NH protons of the ligand disappear and a signal of protons appears at 8.30 ppm. This spectral behavior indicates the formation of metal chelates in which the chelating ligands exist in the azomethine form (**a**) (Scheme 2).

The copper, cobalt, and nickel complexes are paramagnetic. The values of μ_{eff} are 2.09 (**Ia**) and 1.89 μ_B (**IIa**) for the copper complexes, 4.01 (**Ib**) and 4.12 μ_B (**IIb**) for the cobalt complexes, and 3.09 μ_B (**Ic** and **IIc**) for the nickel complexes at room temperature and remain unchanged with the temperature decrease, indicating their mononuclear structure.

The local atomic environment of the metal ions in complexes **I** and **II** (M = Co, Ni, Cu) was studied by XAFS analysis.

The normalized *K*-edge XANES (X-ray Absorption Near Edge Structure) for the copper, nickel, and cobalt complexes (**Ia–Ic**, **IIa–IIc**) are shown in Fig. 2.

As can be seen from Fig. 2, the XANES of complexes **Ib** and **Ic** substantially differ from the XANES of complexes **IIb** and **IIc**, which is manifested in the structure of the first derivatives of these edges and especially in intensities of the pre-edge peak *A*. The first derivative of the Co *K* edge of complex **IIb** has a narrow intense maximum, unlike the first derivative for complex **Ib**, where the latter is split into several maxima. The same tendency is observed for the first derivatives of the Ni *K* edges of complexes **Ic** and **IIc**, although is less pronounced. On going from complexes **Ib** and **Ic** to complexes **IIb** and **IIc**, the XANES exhibits a significant decrease in the intensity of the pre-edge peak *A* reflecting the degree of mixing of the *p–d* atomic orbitals of the metal. These changes in the XANES characteristics are usually assigned to a change in the coordination number and symmetry of the environment of the absorbing atom [42]. Thus, it can be assumed that the transition from **I** to **II** results in the following changes in the nickel and cobalt complexes: the coordination number of the first coordination sphere increases due to the interaction with the nitrogen atoms of the additional azo groups in the

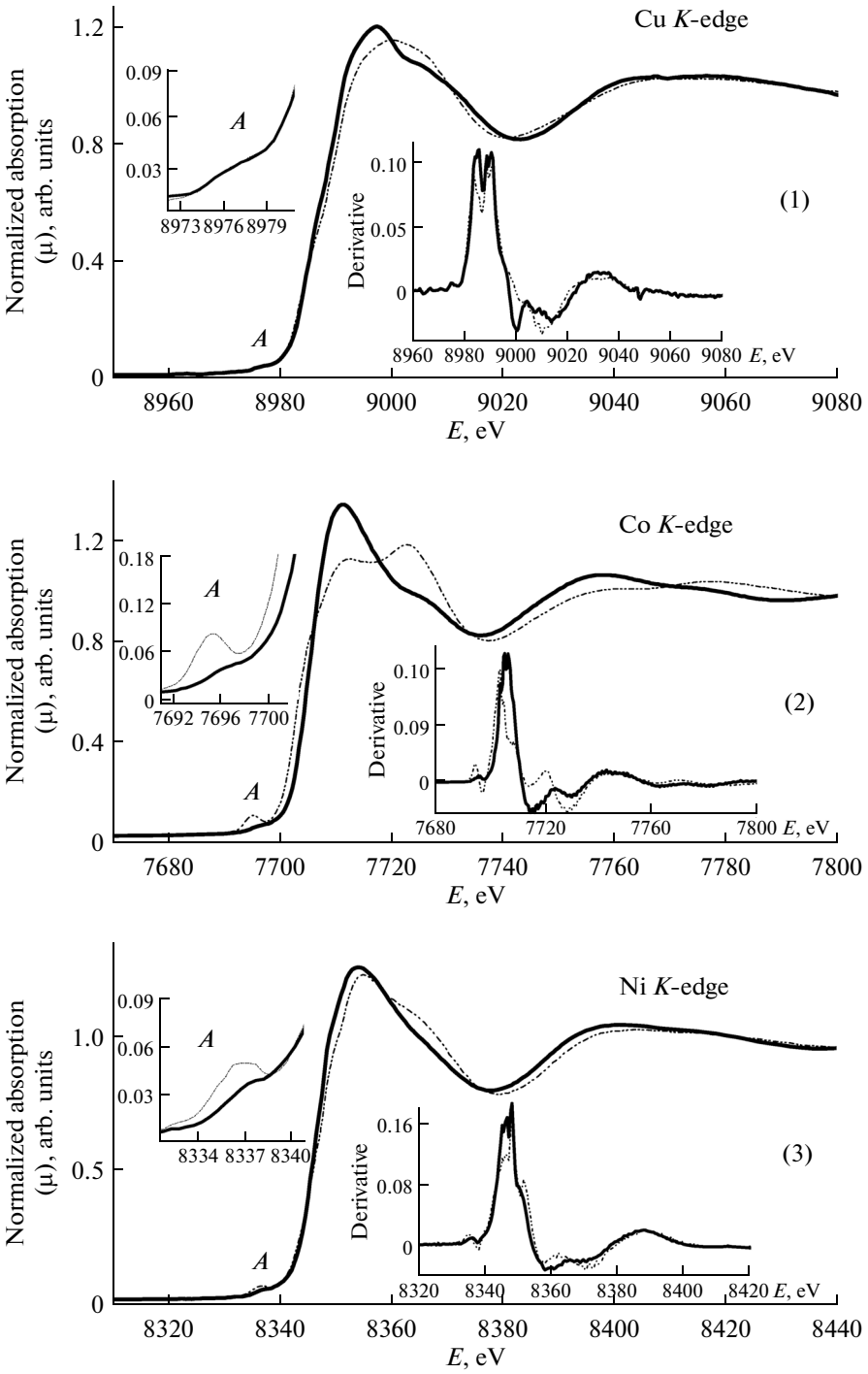

Fig. 2. Normalized *K*-edge XANES for the (1) copper, (2) cobalt, and (3) nickel complexes: (dot) **Ia–Ic** and (solid) **IIa–IIc**. Insets: the regions with the pre-edge peaks *A* and the first derivatives of the edges.

ortho positions in the ligands, and the symmetry of the environment of the metal ions increases.

The first derivatives of the Cu *K* edges for compounds **Ia** and **IIa** have nearly the same splitting, and the characteristics of the pre-edge peak *A* (position and intensities) remain unchanged (Fig. 2). This absorption near-edge structure is characteristic of the copper complexes in which the metal atom has an environment close to tetrahedral, where the degree of distortion is manifested in the value of splitting of the first derivative and the intensity of the pre-edge peak *A*. Thus, the qualitative consideration of the structure of the Cu *K* edges shows no additional interaction of the copper atoms with the atoms of the azo groups of the ligands on going from **Ia** to **IIa**.

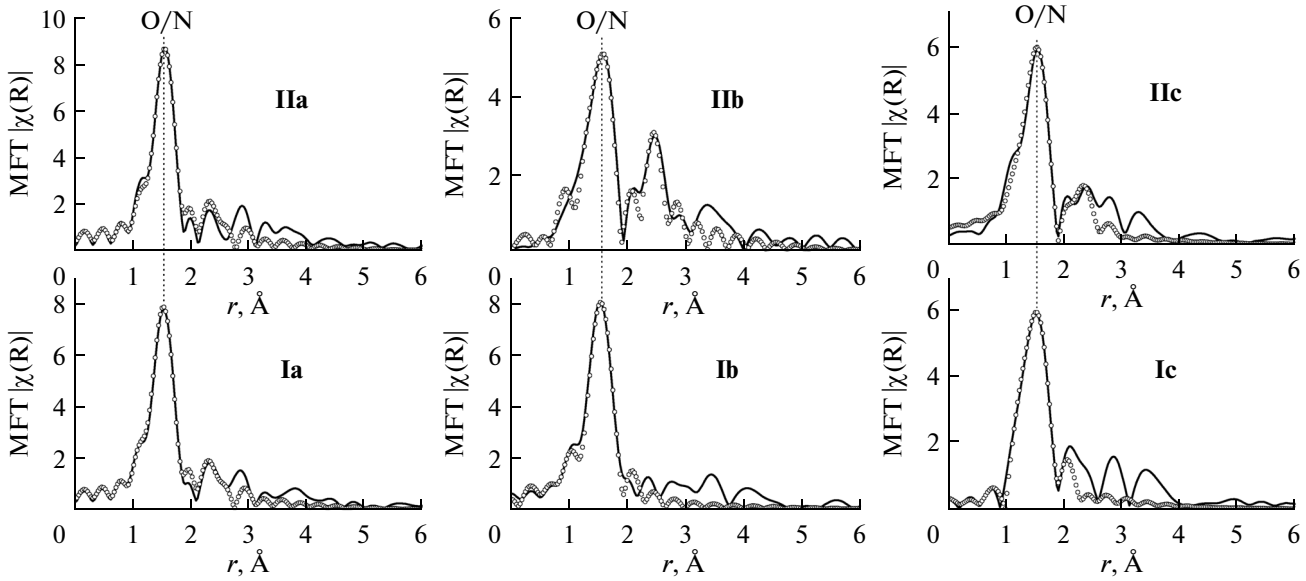

Fig. 3. MFT of the *K*-edge EXAFS for the copper, cobalt, and nickel complexes: **Ia–Ic** and **IIa–IIc** (solid line is experiment, and theory is shown by empty circles).

The quantitative characteristics of the nearest atomic environment of the metal ions in compounds **Ia–Ic** and **IIa–IIc** were obtained from the analysis of the EXAFS of these compounds. The MFT of Cu, Co, and Ni *K*-edge EXAFS of the studied metal chelates are presented in Fig. 3. All MFT contain the main peak at r = 1.51–1.60 Å corresponding to the first nearest coordination sphere consisting of two nitrogen atoms and two oxygen atoms of the ligands and a series of peaks with a small amplitude at long distances r corresponding to the next coordination spheres. The quantitative characteristics for the first coordination sphere obtained by the multisphere nonlinear fitting are given in Table 2.

An analysis of the obtained results (Table 2) shows that the first coordination sphere for the cobalt and nickel ions in compounds **Ib** and **Ic** contains two nitrogen atoms and two oxygen atoms, whereas the total coordination number of the first coordination sphere in complexes **IIb** and **IIc** is six, and the average radius of this coordination sphere increases. These data are well consistent with the qualitative conclusions made by the analysis of the XANES of these compounds. In compounds **Ia** and **IIa**, the parameters of the local atomic environment are close and correspond (to different extents) to the distorted pseudotetrahedral environment of the copper atoms in these compounds.

Thus, the analysis of the *K*-edge XANES and EXAFS showed the octahedral coordination due to additional bonds of the nitrogen atom of this azo group to the metal ion in compounds **IIb** and **IIc** bearing the azo group in the *ortho* position of the amine fragment. For complexes **Ib** and **Ic** in which the azo group is localized in the *para* position, this interaction is sterically hindered and the coordination is close to tetrahedral. In compounds **Ia** and **IIa**, the tetrahedral environment of the copper ion takes place regardless of the type of the ligand.

The results on the local atomic structure of complex **IIb** obtained by XANES are confirmed by the X-ray diffraction data for this complex. The main structural characteristics of complex **IIb** are given in Table 3.

In mononuclear complex **IIb** (Fig. 4), two HL^2 molecules are coordinated to the central metal atom through the tridentate-chelating mode and act as O,N,N-donor ligands. The Co(II) atom is in the distorted octahedral environment of four nitrogen atoms and two oxygen atoms. Each structure includes two five- and two six-membered nonplanar metallocycles.

The groups of atoms O(1)C(1)C(3)C(11) and O(2)C(26)C(28)C(36) in the six-membered metallocycles are planar. The shifts of the N(3) and N(8) atoms from these planes are 0.25(1) and 0.20(2) Å, and the central Co atom shifts from these planes by 0.92(3) and 0.90(3) Å, respectively. The shift of the central metal atom from the mean (±0.2 Å) planes O(1)C(1)C(3)C(11)N(3) and O(2)C(26)C(28)C(36)N(8) in the six-membered metallocycles is 0.70(3) and 0.73(3) Å, respectively. In the case of the five-membered metallocycles, the shift of the central atom from the N(8)C(37)C(38)N(9) plane is 0.56(3) Å, and that from the mean plane N(3)C(12)C(13)N(4) is 0.69(3) Å.

The structural units at the azomethine (C(11)–N(3), C(36)–N(8)) and azo (N(4)–N(5), N(9)–N(10)) groups exist in the *trans* configuration. The torsion angles C(3)C(11)N(3)C(12) and

Table 2. Structural data (obtained from EXAFS*) for the local atomic environment of Cu, Co, and Ni in compounds **I** and **II**

Compound	*N*	*R*, Å	σ^2, Å^2	Atoms of coordination sphere	*Q*, %
Ia	2	1.93	0.0038	O/N	2.0
	2	1.98	0.0038	O/N	
IIa	2	1.94	0.0030	O/N	3.0
	2	2.00	0.0030	O/N	
Ib	2	1.96	0.0030	O/N	0.5
	2	1.99	0.0030	O/N	
IIb	2	2.03	0.0030	O/N	4.0
	2	2.09	0.0030	O/N	
	2	2.26	0.0030	O/N	
Ic	2	1.94	0.0034	O/N	8.6
	2	1.98	0.0034	O/N	
IIc	2	1.97	0.0038	O/N	2.4
	2	2.03	0.0038	O/N	
	2	2.10	0.0038	O/N	

* *R* are the interatomic distances, *N* is the coordination number, σ^2 is the Debye–Waller factor, and *Q* is the decoupling function.

Table 3. Selected interatomic distances (*d*) and bond angles (ω) in the structure of complex **IIb** and interatomic distances in molecule HL^2

IIb				HL^2	
Bond	*d*, Å	Bond	*d*, Å	Bond	*d*, Å
N(1)–N(2)	1.401(2)	N(6)–N(7)	1.403(2)	N(1)–N(2)	1.409(6)
C(1)–O(1)	1.267(2)	C(26)–O(2)	1.269(2)	C(9)–O(1)	1.228(6)
C(11)–N(3)	1.312(2)	C(36)–N(8)	1.323(2)	C(10)–N(3)	1.335(7)
N(4)–N(5)	1.2668(19)	N(9)–N(10)	1.2695(19)	N(4)–N(5)	1.260(5)
Co(1)–O(1)	2.0921(12)	Co(1)–O(2)	2.0990(12)		
Co(1)–N(3)	2.0337(14)	Co(1)–N(8)	2.0290(15)		
Co(1)–N(4)	2.2510(14)	Co(1)–N(9)	2.2889(15)		
Angle	ω, deg	Angle	ω, deg		
O(1)Co(1)N(4)	167.09(6)	O(2)Co(1)N(9)	167.53(5)		
N(3)Co(1)N(8)	175.41(6)	O(2)Co(1)N(8)	91.00(5)		
O(1)Co(1)N(3)	90.87(5)	O(1)Co(1)N(8)	91.88(5)		
O(1)Co(1)O(2)	83.89(5)	O(1)Co(1)N(9)	98.12(5)		
N(4)Co(1)N(3)	76.94(6)	N(4)Co(1)N(8)	100.02(6)		
N(4)Co(1)N(9)	79.97(5)	N(4)Co(1)O(2)	100.75(5)		
N(3)Co(1)O(2)	92.95(6)	N(3)Co(1)N(9)	99.31(6)		
N(5)Co(1)N(9)	76.66(6)				

C(28)C(36)N(8)C(37), C(13)N(4)N(5)C(19) and C(38)N(9)N(10)C(44) are characterized by values of 170.55(7)° and 175.33(7)°, 172.89(7)° and 171.51(5)°, respectively. The bond lengths and angles in two ligand fragments are close but not equal, unlike the isostructural azo complex described previously [34].

Thus, the complexes with different structures are formed depending on the metal nature and ligand structure. In the case of the Co(II) and Ni(II) com-

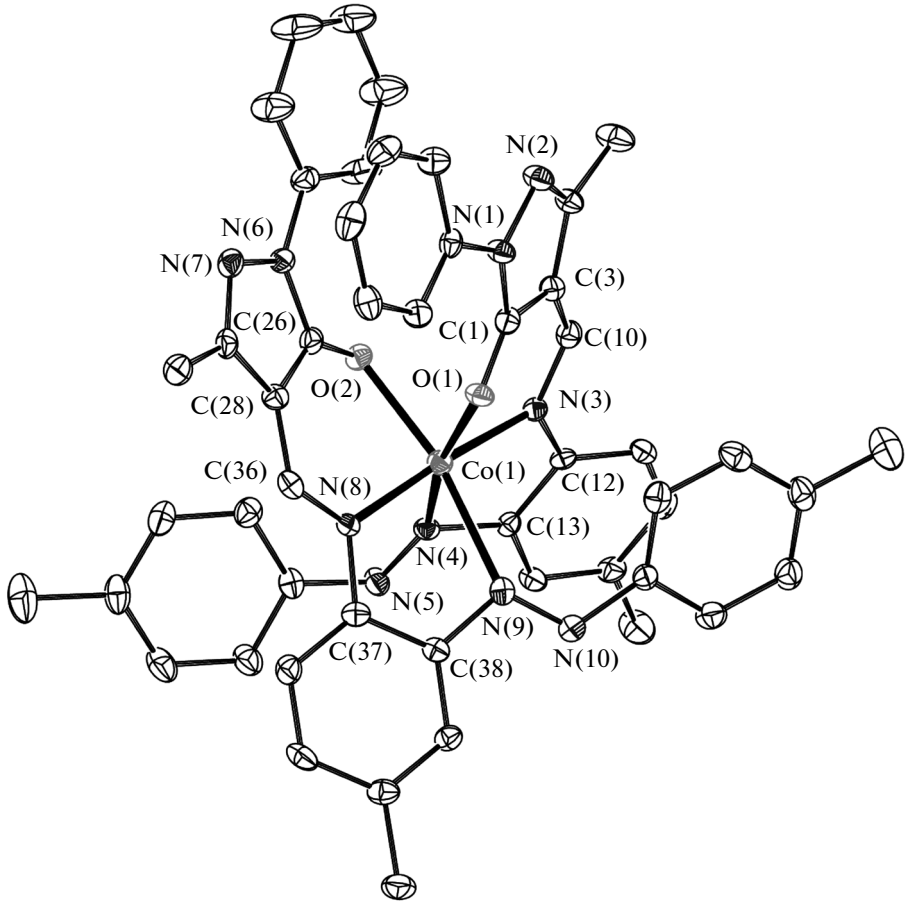

Fig. 4. Structure of complex **IIb** in the representation of atoms by 50% probability atomic displacement ellipsoids (hydrogen atoms are omitted).

plexes, the presence of the azo group in the *ortho* position of the amine fragment of the azomethine ligand results in the formation of two five- and two six-membered nonplanar metallocycles in the distorted octahedral environment of the metal atom and the participation of the nitrogen atom of the azo group in coordination. If the azo group is in the *para* position of the amine fragment, its coordination to the metal does not occur and structures with two six-membered metallocycles are formed.

For the copper complexes, the azo groups are not involved in coordination, regardless of their position, and the structures with two six-membered metallocycles are formed.

ACKNOWLEDGMENTS

The IR and ^{1}H NMR spectra were recorded using the equipment of the TsKP Molekulyarnaya spektroskopiya. The equipment of the Unique Research System "Kurchatov Synchrotron Radiation Source" financed by the Ministry of Education and Science of the Russian Federation (project identifier RFMEFI61914X0002) was used.

This work was supported by the Russian Foundation for Basic Research, projects nos. 13-03-12418 ofi-m, 14-03-31419 mol_a.

REFERENCES

1. Hernandez-Molina, R. and Mederos, A., in *Comprehensive Coordination Chemistry II*, Lever, A.B.P, Ed., Amsterdam–Oxford–New York: Elsevier–Pergamon, 2003, vol. 1, p. 411.
2. Garnovskii, A.D. and Vasil'chenko, I.S., *Usp. Khim.*, 2002, vol. 71, no. 11, p. 1064.
3. *Synthetic Coordination and Organometallic Chemistry*, Blanco, L.M., Garnovskii, A.D., Garnovskii, D.A., et al., Eds., New York: Marcel Dekker, 2003.
4. Vigato, P.A., Tamburini, S., and Bertelo, L., *Coord. Chem. Rev.,* 2007, vol. 251, no. 11, p. 1311.
5. Vigato, P.A., Tamburini, S., and Bertelo, L., *Coord. Chem. Rev.*, 2008, vol. 252, nos. 18–20, p. 1871.
6. Vigato, P.A. and Tamburini, S., *Coord. Chem. Rev.*, 2004, vol. 248, nos. 17–20, p. 1717.

7. Garnovskii, A.D. and Vasil'chenko, I.S., *Usp. Khim.*, 2005, vol. 71, no. 3, p. 211.
8. Garnovskii, A.D., Vasilchenko, I.S., Garnovskii, D.A., and Kharisov, I.S., *J. Coord. Chem.*, 2009, vol. 62, no. 2, p. 151.
9. Garnovskii, A.D., Vasil'chenko, I.S., Garnovskii, D.A, et al., *Ross. Khim. Zh.*, 2009, vol. 53, no. 1, p. 100.
10. Gatteschi, D., Sessoli, R., and Cornia, A., in *Comprehensive Coordination Chemistry II*, Lever, A.B.P, Ed., Amsterdam–Oxford–New York: Elsevier–Pergamon, 2003, vol. 2, p. 393.
11. Tompson, K.L., *Coord. Chem. Rev.*, 2005, vol. 249, no. 23, p. 2549.
12. *Organic Light-Emmiting Devices*, Mueller, K. and Schert, U, Eds.,. Weinheim–New York: Wiley–VCH, 2006, p. 94.
13. Burdette, S.C. and Lippard, S.J., *Coord. Chem. Rev.*, 2001, vols. 216–217, p. 333.
14. Bren', V.A., *Usp. Khim.*, 2001, vol. 70, no. 12, p. 1152.
15. Ushakov, E.N., Alfimov, M.V., and Gromov, S.P., *Usp. Khim.*, 2008, vol. 77, no. 1, p. 39.
16. Halcrow, M.A.,*Comprehensive Coordination Chemistry II*, Que, L. and Tolman, W.B., Eds., New York: Elsevier–Pergamon, 2003, vol. 8, p. 395.
17. *Ross. Khim. Zh.*, 2004, vol. 48, no. 4176 p.
18. *Spin Crossover in Transition Metal Compounds.*, Gütlich, P. and Goodwin, H.A., Eds., Topics in Curr. Chem., vols. 233–235, Berlin: Springer, 2004.
19. Sato, O., Tao, J., and Zhang, Y.-Z., *Angew. Chem., Int. Ed. Engl.*, 2007, vol. 46, p. 2152.
20. Nihei, M., Shiga, T., Maeda, Y., and Oshio, H., *Chem. Rev.*, 2007, vol. 251, p. 2606.
21. Weber, B., *Coord. Chem. Rev.*, 2009, vol. 253, p. 2432.
22. Gütlich, P., Garcia, Y., and Woike, T., *Coord. Chem. Rev.*, 2001, vols. 219–221, p. 839.
23. Klajn, R., Wesson, P.J., Bishop, K.J.M., and Grzybowski, B.A., *Angew. Chem., Int. Ed. Engl.*, 2009, vol. 48, no. 38, p. 7035.
24. Porai-Koshits, B.A. and Kvitko, I.Ya., *Zh. Obshch. Khim.*, 1962, vol. 32, no. 12, p. 4050.
25. Chernyshov, A.A., Veligzhanin, A.A., and Zubavichus, Y.V., *Nucl. Instr. Meth. Phys. Res. A*, 2009, vol. 603, p. 95.
26. Kochubei, D.I., Babanov, Yu.A., Zamaraev, K.I., et al., Novosibirsk: Nauka, Sib. Otd., 1988, 306 p.
27. Newville, M., *J. Synchrotron Radiat.*, 2001, vol. 8, p. 96.
28. Zabinski, S.I., Rehr, J.J., Ankudinov, A., and Alber, R.C., *Phys. Rev. B: Condens. Matter Mater. Phys.*, 1995, vol. 52, p. 2995.
29. *SMART (Control) and SAINT (Integration) Software. Version 5.0*, Madison (WI, USA): Bruker AXS Inc., 1997.
30. Sheldrik, G.M., *SADABS. Program for Scanning and Correction of Area Detector Data,* Göttingen: Univ. of Göttingen, 1997.
31. *SHELXS-97 and SHELXL-97,* Göttingen: Univ. of Göttingen, 1997.
32. Spek, A.L., *J. Appl. Crystallogr.*, 2003, vol. 36, p. 7.
33. Weber, B., *Coord. Chem. Rev.,* 2009, vol. 253, p. 2432.
34. Burlov, A.S., Mashchenko, S.A., Antsyshkina, A.S., et al., *Russ. J. Coord. Chem.*, 2013, vol. 39, no. 12, p. 707.
35. Burlov A.S., Mashchenko, S.A. Vlasenko, V.G., et al., *J. Mol. Struct.,* 2014, vol. 1061, p. 47.
36. Garnovskii, A.D., Burlov, A.S., Starikov, A.G., et al., *Russ. J. Coord. Chem.*, 2010, vol. 36, no. 7, p. 479.
37. Burlov, A.S., Nikolaevskii, S.A., and Bogomyakov, A.S., *Russ. J. Coord. Chem.,* 2009, vol. 35, no. 7, p. 486.
38. Kurkovskaya, L.N, Shapet'ko, N.N., Kvitko, I.Ya., et al., *Zh. Org. Khim.,* 1973, vol. 9, no. 4, p. 821.
39. Antsyshkina, A.S., Sadikov, G.G., Uraev, A.I., et al., *Kristallografiya*, 2000, vol. 45, no. 5, p. 850.
40. Burlov, A.S., Uraev, A.I., Garnovskii, D.A., et al., *J. Mol. Stuct.*, 2014, vol. 1064, p. 111.
41. Allen, F.H., Kennard, O., Watson, D.G., et al., *J. Chem. Soc., Perkin Trans.*, 1987, no. 12, p. S1.
42. Yamamoto, T., *X-ray Spectrom.*, 2008, vol. 37, p. 572.

Translated by E. Yablonskaya